Preparation and characterization of macroporous chitosan/wollastonite composite scaffolds for tissue engineering

LI ZHAO, JIANG CHANG*
Biomaterials and Tissue Engineering Research Center, Shanghai Institute of Ceramics, Chinese Academy of Sciences, 1295 Dingxi Road, Shanghai 200050, P.R. China
E-mail: jchang@mail.sic.ac.cn

Chitosan/wollastonite composite scaffolds were prepared by a thermally induced phase separation method. The microstructure, mechanical performance and *in vitro* bioactivity of the composite scaffolds were investigated. The composite scaffolds were macroporous and wollastonite particles were dispersed uniformly on the surface of the pore walls. Scanning electron microscope images of the composite scaffolds demonstrated that the scaffolds had interconnected pores with diameters from 60 to 200 μm. Both the pore size and structure were affected by freezing temperature. The mechanical performance of the composite scaffolds was improved compared to that of pure chitosan scaffolds. The *in vitro* bioactivity of the scaffolds was evaluated by soaking samples in simulated body fluid and the apatite layer was observed on the surface of the pore walls of the composite scaffolds. Our results suggest that the incorporation of wollastonite into chitosan could enhance both the mechanical strength and the *in vitro* bioactivity of the resultant composite. The macroporous chitosan/wollastonite scaffolds may be a potential candidate for application in tissue engineering.

1. Introduction

Tissue engineering is a newly emerging biomedical technique that involves the artificial manipulation of cells to promote tissue and organ regeneration [1]. Biodegradable scaffolds act as a critical part in tissue engineering, and three-dimensional (3D) scaffolds provide the necessary support for cells to proliferate and maintain their differentiated functions. At present, several scaffold materials have been investigated for tissue engineering bone and cartilage, including hydroxyapatite (HAP), poly(α-hydroxyester), and natural polymers such as collagen and chitin [2].

Recently, much attention has been given to utilize chitosan in biomedical applications, such as wound dressings, drug delivery systems, space-filling implants, and tissue engineering [3]. Chitosan is the product obtained from the deacetylation of the natural biopolymer chitin. The presence of free amine groups in chitosan enhances the greater solubility and reactivity of this polymer than that of chitin [4]. The surface of chitosan is hydrophilic, which facilitates cell adhesion, proliferation, and differentiation [5], Despite its otherwise attractive properties, porous chitosan scaffolds are lack of mechanical strength and may not be suitable for tissue engineering of hard tissue [3]. For solving this problem, an important strategy is to combine chitosan with inorganic materials so that the resulting hybrid materials possess improved mechanical and biological properties. Many inorganic materials including calcium carbonate, calcium phosphate and silica have been studied for preparation of chitosan-inorganic composites [6]. Wollastonite is a naturally occurring calcium silicate, which is bioactive and can induce HAP formation on the surface after immersion in simulated body fluid (SBF) [7, 8]. Other reports have shown that the incorporation of wollastonite into poly(butylene terephthalate) could remarkably enhance mechanical strength of the composites [9]. In the present study, we report on preparation and characterization of chitosan scaffolds reinforced by wollastonite through a thermally induced phase separation method.

2. Experimental

2.1. Materials

Chitosan ($\geq 91.29\%$ deacetylated) was obtained from Shanghai Cabo Industrial Trade Corporation. Wollastonite powder was prepared by a chemical coprecipitation method. In short, an aqueous solution of Na_2SiO_3 was added dropwise to a $Ca(NO_3)_2$ solution,

*Author to whom all correspondence should be addressed.

and after being mixed, the reaction solution was stirred overnight at room temperature, and left for another 12 h at room temperature without stirring. The wollastonite precipitates were filtered and washed first with deionized water and subsequently with absolute ethyl alcohol. The obtained powders were dried at 100 °C for 24 h and then sintered at 800 °C for 2 h.

2.2. Preparation of porous chitosan/wollastonite composite scaffolds

A solution of 2 wt % chitosan was prepared by dissolving chitosan in 0.2 M acetic acid aqueous solution. Wollastonite powders with particle size from 100 to 250 nm were added to the prepared solution, the mixture was stirred overnight at room temperature, and then transferred into a refrigerator at a preset freezing temperature (− 20 °C or − 80 °C) to solidify the solvent. The solidified mixture was maintained at the preset temperature for at least 8 h, and then transferred into a freeze-dryer and lyophilized. Different compositions of the composites were obtained by controlling the wollastonite content in the mixture.

2.3. Characterization of composite scaffolds

The porosities of the composite scaffolds were determined with a liquid displacement method [10, 11]. Microstructural characterization of the scaffold structure was carried out using a Shimadzu 8705QH$_2$ electron probe microanalyzer (EPMA) (Shimadzu Co., Japan) equipped with an energy dispersive spectrometer (EDS) (Oxford Instruments Co., UK) at an accelerating voltage of 20 kV. Before observation, the composite scaffolds were sputter-coated with gold under an argon atmosphere. For mechanical testing, composite discs with the dimension of 13 mm in diameter and 5 mm in thickness were prepared, and the compressive strength was conducted using an AG-1 Shimadzu mechanical tester (Shimadzu Co., Japan). The crosshead speed was 0.5 mm/min, and the value of the compressive strength was the average of three test results.

2.4. Soaking in SBF

For characterization of the *in vitro* bioactivity, samples were soaked in SBF for different time periods. The simulated body fluid, with ion concentration nearly equal to those of human blood plasma for apatite nucleation, was prepared according to the method proposed by Kokubo *et al*. [12]. The circular discs of the scaffolds with the dimension of 12 mm in diameter and 3 mm in thickness were immersed in 35 ml SBF solution at 37 °C without stirring. After immersion for various time periods, the samples were removed from the SBF solution, rinsed in deionized water, and lyophilized. The morphology and composition of the newly formed particles on the surface of the samples were analyzed with a JSM-6700F field emission scanning electron microscope (FESEM) (JEOL Co., Japan) and EDS.

2.5. Statistic analysis

Mechanical testing was analyzed using the Student's *t*-test (assuming two-tailed, unpaired data). Differences were considered significant when $p < 0.05$.

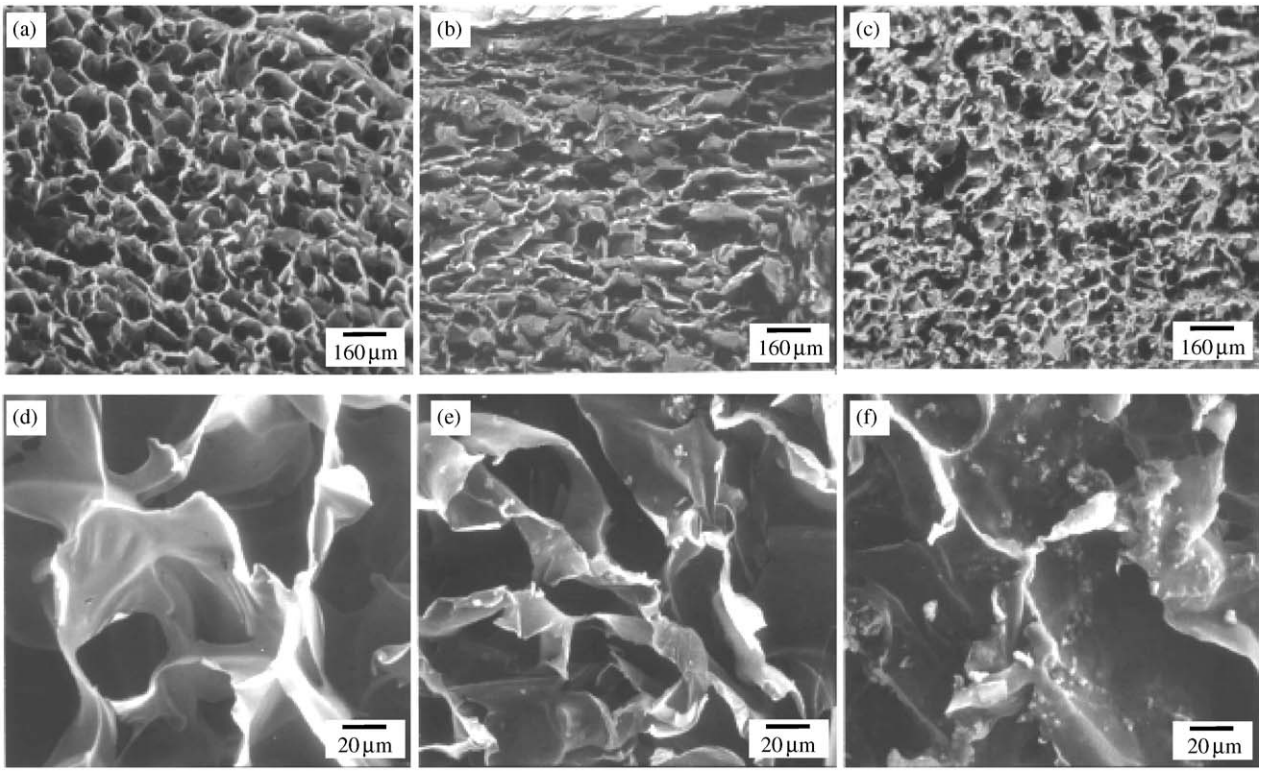

Figure 1 SEM micrographs of chitosan/wollastonite composite scaffolds with different chitosan/wollastonite weight ratio: (a, d) 100/0, (b, e) 90/10, and (c, f) 50/50.

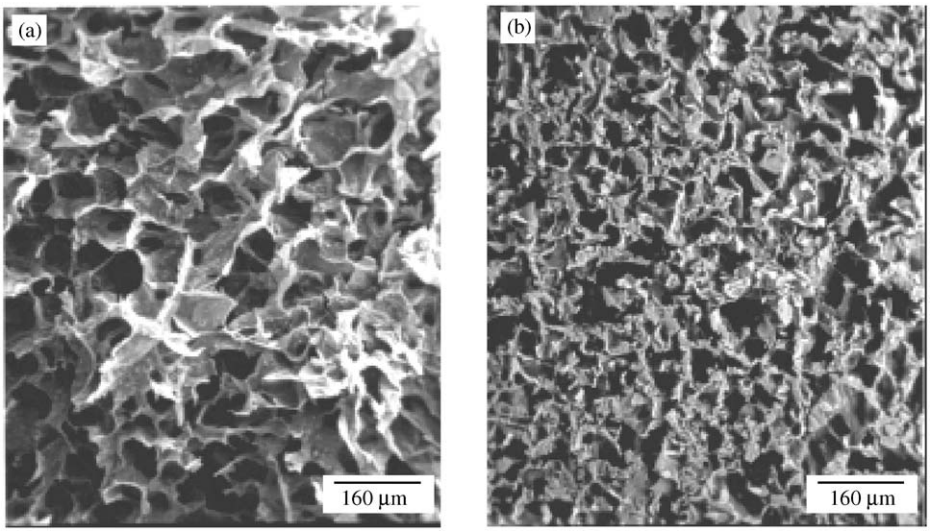

Figure 2 SEM micrographs of chitosan/wollastonite composite scaffolds with weight ratio of 50/50 prepared by different freezing temperature: (a) − 20 °C, (b) − 80 °C.

3. Results

The 3D chitosan/wollastonite composite scaffolds were prepared using a thermally induced phase separation method. Fig. 1 shows SEM photographs of the cross sections of the composite scaffolds. The scaffolds exhibited a macroporous structure with interconnected open pores. The pore size varied from 60 to 200 μm, and high magnification SEM images (Fig. 1(e), (f)) showed that the wollastonite particles were dispersed uniformly on the pore walls of the composite scaffolds. With the increase of wollastonite content, pore structure became irregular. When the wollastonite content increased to more than 50 wt % of the composite, the macroporous structural integrity of the composite scaffolds could not be maintained (data not shown).

The densities and porosities of the composite scaffolds are listed in Table I. It is obvious that the densities of the composite scaffolds increased with the increase of the wollastonite content, while the porosities of the scaffolds decreased.

Fig. 2 shows the effect of freezing temperature on the microstructure of the composite scaffolds. The scaffolds prepared at − 20 °C exhibited larger pores, while scaffolds prepared at − 80 °C exhibited smaller pores. However, freezing temperature does not have obvious effects on the porosity of the chitosan/wollastonite composite scaffolds as seen in Table I.

TABLE I Densities and porosities of chitosan/wollastonite composite scaffolds

Composition	Freezing temperature (°C)	Density (g/cm^2)	Porosity (%)
Chitosan	− 20	0.052	92.56
C9W1	− 20	0.0553	91.65
C7W3	− 20	0.0726	87.48
C5W5	− 20	0.0993	85.6
Chitosan	− 80	0.0371	92.41
C9W1	− 80	0.0446	89.98
C7W3	− 80	0.0608	88.17
C5W5	− 80	0.127	81.85

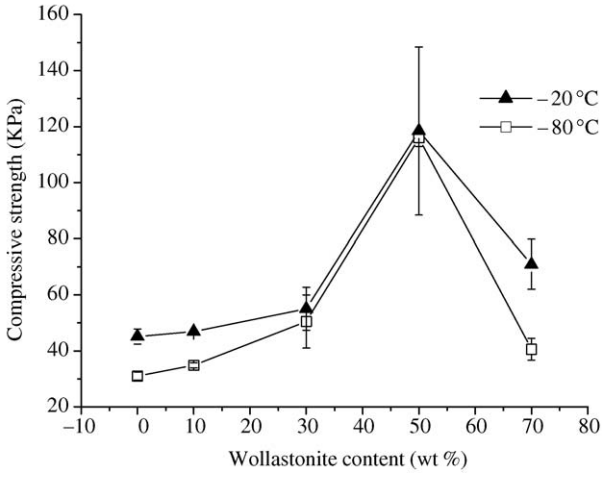

Figure 3 Compressive strength of chitosan/wollastonite composite scaffolds as a function of wollastonite content at different freezing temperatures.

Fig. 3 shows the compressive strength of the composite scaffolds. It is clear to see that the compressive strength of the composite scaffolds increased as the wollastonite content increased, reaching a maximum at 50 wt %, and then decreased with further increase of the wollastonite content. There were no significant differences in the compressive strength between different freezing temperatures.

Fig. 4(a)–(e) shows the SEM micrographs of the chitosan/wollastonite composite scaffolds with the weight ratio of 50/50 before and after soaking in SBF at 37 °C. Fig. 4(f) shows the EDS spectrum of the composite scaffolds after soaking for 3 weeks. It is obvious that surface morphology of the composite scaffolds was changed and new particles were deposited uniformly on the surface of the pore walls. The high magnification SEM micrograph (Fig. 4(e)) indicated that the newly formed particles showed a typical HAP morphology, and the EDS analysis showed that the particles were mainly composed of calcium and phosphorus and the Ca/P molar ratio was close to that of HAP.

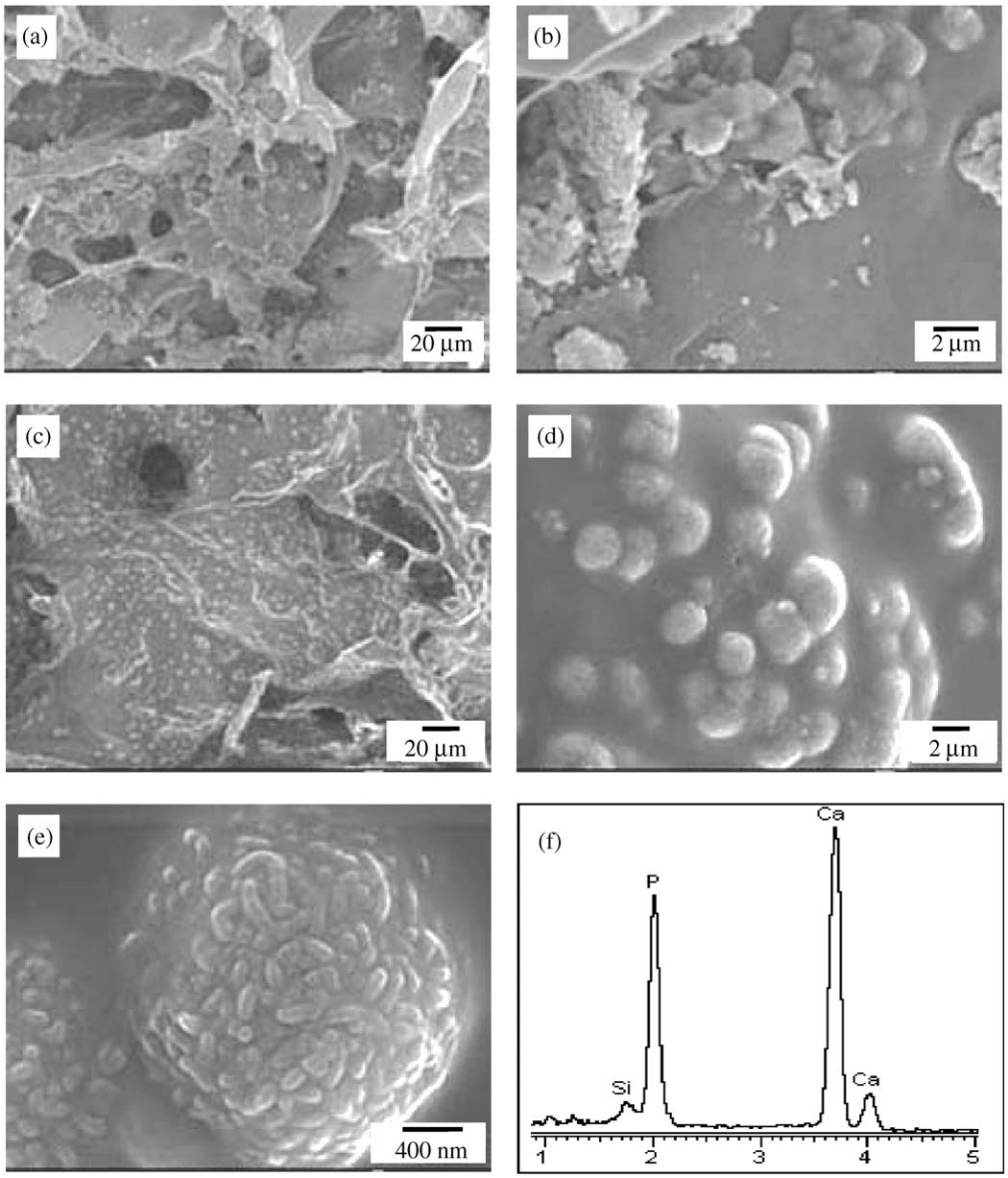

Figure 4 SEM micrographs of chitosan/wollastonite composite scaffolds with weight ratio of 50/50 soaked in SBF for various period times: (a, b) 0 day, (c, d, e) 3 weeks, and (f) EDS spectrum of the composite scaffolds after soaking in SBF for 3 weeks.

4. Discussion

The scaffolds were prepared by a solid–liquid phase separation method. The solid–liquid phase separation is attributed to the crystallization of the solvent. When the chitosan solution was frozen, the solvent began to crystallize. The crystallization of the solvent pushed chitosan to the crystallization front as ''impurities'' [10]. After the solvent crystals had been sublimated, the 3D scaffolds were formed with pores, similar to the geometry of solvent crystals. When wollatonite was introduced into the chitosan solution, both chitosan and wollastonite particles were expelled from the crystallization front, forming a chitosan/wollastonite-rich phase. After sublimation of the solvent, this chitosan/wollastonite-rich phase formed a continuous skeleton for the chitosan/wollastonite scaffolds, and the spaces taken by solvent crystals became pores of the scaffold. On the other hand, the existence of wollastonite particles perturbed the crystallization of solvent. The randomly distributed wollastonite particles changed the solvent crystallization front by impeding the crystal growth, making the crystals of the solvent more irregular. As a result, the composite scaffolds exhibited irregular pore structure as compared to pure chitosan scaffolds. However, on the whole, wollastonite particles were dispersed uniformly in the scaffolds.

Freezing temperature affected the microstructure of the chitosan/wollastonite composite scaffolds greatly, as shown in Fig. 2. The scaffolds prepared at lower freezing temperature ($-80\,^{\circ}C$) showed a smaller pore size. The explanation for this phenomenon is that more solvent crystals nucleated simultaneously at the high cooling rate, which resulted in an increase of the number of pores and a decrease of the pore size. At the low cooling rate, the solvent crystals had enough time to grow, which resulted in the formation of large pores.

The incorporation of wollastonite into chitosan scaffolds caused a significant improvement in compressive strength of the composites. According to the mechanism of the mechanical reinforcement postulated by some researchers [11], not only was there a physical bond between wollastonite and the chitosan matrix, but potentially a chemical reaction between the chitosan, solvent, and wollastonite due to the high surface charge

density of chitosan and its ability to form ionic complexes. However, when the wollastonite content exceeded 50 wt % of the composite, further incorporation of wollastonite particles strongly perturbed the crystallization of the solvent during the freezing process, which resulted in the structural integrity being damaged and a dramatic decrease of the mechanical strength taking place. Our results suggested that the weight ratio of 50/50 was the optimal composition for the chitosan/wollastonite composites.

SBF immersion results showed the formation of apatite on the surface of the pore walls after 3 weeks of soaking. A previous study [11] has shown that pure chitosan could not induce apatite formation after soaking in SBF. Therefore, our results suggested that the incorporation of wollastonite into chitosan matrix could enhance the *in vitro* bioactivity of the composite scaffolds. The mechanism of HAP formation on wollastonite has been studied by de Aza and his coworkers [13]. The study suggested that Ca^{2+} release and ionic interchange of Ca^{2+} for $2H^{+}$ could result in the formation of an amorphous silica layer on the surface of wollastonite, which provided a favorable site for HAP nucleation. In the chitosan/wollastonite composite scaffolds, although the wollastonite particles were imbedded in the chitosan matrix, the microporous structure of the chitosan matrix still allowed release of Ca^{2+} and supported HAP deposition. A previous study has shown that chitosan/β-TCP composites could also induce HAP formation in SBF after 4 weeks of soaking [11]. In comparison to the composite scaffolds composed of chitosan and β-TCP, our results showed faster HAP formation, which appeared after 3 weeks of soaking in SBF. This study suggested that the incorporation of wollastonite into chitosan not only mechanically reinforced the scaffold, but also enhanced the *in vitro* bioactivity of the materials.

5. Conclusions

Macroporous chitosan/wollastonite composite scaffolds were prepared by a thermally induced phase separation method. The wollastonite particles were uniformly dispersed on the pore walls of the composite scaffolds. The pore size of the composite scaffolds was affected by freezing temperatures and a lower freezing temperature resulted in a smaller pore size. The compressive strength of the scaffolds was significantly improved after the addition of wollastonite. An apatite layer was formed on the surface of the composite scaffolds after soaking in SBF, which indicated that the addition of wollastonite to the chitosan matrix enhanced the bioactivity of the scaffolds. It is expected that the desirable structure and properties can be achieved via the adjustment of the chitosan/wollaslonite ratio and the composite preparation temperature.

Acknowledgments

This work was supported by grants from the National Science Foundation (50142003) and the Shanghai Science Foundation (01ZE14003).

References

1. Y. TABATA, *Drug. Discov. Today* **6** (2001) 483.
2. D. W. HUTMACHER, *Biomaterials* **21** (2000) 2529.
3. Y. ZHANG and M. Q. ZHANG, *J. Biomed. Mater. Res.* **61** (2002) 1.
4. O. A. C. MONTEIRO and C. AIROLDI, *Int. J. Biol. Macromol.* **26** (1999) 119.
5. S. V. MADIHALLY and H. W. T. MATTHEW, *Biomaterials* **20** (1999) 1133.
6. C. MUZZARELLI and R. A. A. MUZZARELLI, *J. Inorg. Biochem.* **92** (2002) 89.
7. P. SIRIPHANNON, Y. KAMESHIMA, A. YASUMORI, K. OKADA and S. HAYASHI, *J. Eur. Ceram. Soc.* **22** (2002) 511.
8. X. LIU, C. DING and Z. WANG, *Biomaterials* **22** (2001) 2007.
9. M. RISBUD, D. N. SAHEB, J. JOG and R. BHONDE, *ibid.* **22** (2001) 1591.
10. R. Y. ZHANG and P. X. MA, *J. Biomed. Mater. Res.* **44** (1999) 446.
11. Y. ZHANG and M. Q. ZHANG, *ibid.* **55** (2001) 304.
12. T. KOKUBO, H. KUSHITANI and S. SAKKA, *ibid.* **24** (1990) 721.
13. P. N. DE AZA, F. GUITIAN and S. DE AZA, *Script. Metal. Mater.* **31** (1994) 1001.

Received 8 May
and accepted 10 September 2003